https://doi.org/10.15407/knit2024.01.003
UDC 533.6.013.14 : 629.1.025.3

N. S. PRYADKO, Prof., Doctor Tech. Sci., Leading Researcher
ORCID 0000-0003-1656-1681
E-mail: np-2006@ukr.net
H. O. STRELNIKOV, Prof., Doctor Tech. Sci., Head of Department
ORCID 0000-0001-9810-1966
E-mail: strelaga38@ukr.net
K. V. TERNOVA, PhD, Senior Researcher
ORCID 0000-0001-9560-5827
E-mail: ternovayakaterina@gmail.com

Institute of Technical Mechanics of the National Academy of Sciences of Ukraine and State Space Agency of Ukraine
15 Leshko-Popelia Str., Dnipro, 49005 Ukraine

RESEARCH OF SUPERSONIC FLOW IN SHORTENED NOZZLES OF ROCKET ENGINES WITH A BELL-SHAPED TIP

The flow in a shortened nozzle with a bell-shaped tip is considered. A comparison of the wave structures of the supersonic gas flow in shortened nozzles with short and long tips formed by compression and stretching of the original bell-shaped nozzle for connection, respectively, with the long and short conical part of the base nozzle at the same nozzle length was carried out. Under operation conditions at sea level and low pressure at the nozzle inlet ($P_0 < 50 \cdot 10^5$ Pa), a large-scale vortex structure, starting from the corner point of the nozzle inlet, is observed in both nozzles. In addition, in the long tip, a small-scale vortex is observed on the wall near its cut. A barrel-shaped wave structure of hanging jumps with a closing Mach disc is formed in the flow in both nozzles, inside which a "saddle-shaped" wave structure of low intensity is noticed. In the separation flow in the tip (when $P_0 < 50 \cdot 10^5$ Pa and $P_н = 1 \cdot 10^5$ Pa), the pressure on the wall in the separation zone is slightly lower (by ≈ 5-10%) than the external pressure $P_н$. When the engine is operating in the upper layers of the atmosphere, the static pressure on the section of both tips is proportional to the pressure at the entrance of the nozzle. In the cross-section, starting from the axis of the nozzle to ~0.89 R/R_a (the ratio of the current value of the radius R to the radius of the nozzle wall at the outlet R_a), the pressure decreases to a value proportional to the pressure at the nozzle inlet. Then, it increases linearly to the value of the pressure on the tip wall, which is proportional to the pressure at the nozzle inlet. This is due to the wave structure of the flow inside the nozzle. It was established that with a decrease in the length of the nozzle conical part, the impulse coefficient of the nozzle decreases significantly for operating at sea level and slightly decreases for operating in the upper layers of the atmosphere. The results of calculations correlate satisfactorily with the experimental study results of the flows in shortened nozzles with a bell-shaped tip.

***Keywords*:** *shortened nozzle, tip, supersonic flow, pressure, wave structure, impulse.*

Цитування: Pryadko N. S., Strelnikov H. O., Ternova K. V. Research of supersonic flow in shortened nozzles of rocket engines with a bell-shaped tip. *Space Science and Technology.* 2024. **30**, № 1 (146). P. 3—13. https://doi.org/10.15407/knit2024.01.003

INTRODUCTION

In rocket and space engineering, much attention is paid to the study of flows in the rocket engine nozzles of various shapes. The nature of the subsonic and supersonic flow in the nozzle affects the characteristics of the engine and the rocket as a whole. To increase the power characteristics of the engine installation, it is necessary to optimize the characteristics of the nozzle for different operating conditions. For this, the nozzle designer must have information about the characteristics of various nozzle configurations.

Laval classic nozzles are widely known and well-researched. In [13], optimal shockless unshorted Laval nozzles are studied. Papers [6, 16, 17] consider shortened profiles of round supersonic nozzles. In recent years, nozzles with an unconventional contour, the so-called "dual bell nozzle" [1, 4, 18], are attracting increasing attention, the research of which is carried out using modern simulation software and modern experiments. Such nozzles were studied earlier [15, 19, 23]. At the same time, it was necessary to consider the features of inherent flow in such nozzles, in particular, the separation currents in them. In the work of Volkov and Yemelyanov [3], dual bell nozzles are considered from the point of view of their application to increase the expansion degree of the nozzle and its specific impulse. In works [7, 9], separation flows in similar nozzles were investigated. The calculation results of the shock wave structure of the flow in this type of nozzle agreed with the experiment [5, 14]. Studies of various turbulence models in relation to non-traditional nozzles of the "dual bell nozzle" type were carried out in [8]. Work [24] showed a weak effect of gas properties on the calculated pressure distribution along the nozzle wall. To study the influence of flow regimes at the separation of the free jump of the compression on the wave structure of the flow [2], an experimental study of the unsteady flow in a parabolic nozzle under certain operating conditions (in terrestrial and void conditions) was carried out.

To calculate the flow in traditional Laval nozzles, the characteristic method was most often used. Unlike laminar flows, the calculation of which is no longer complicated by modern application software packages, determining the characteristics of turbulent flows for several reasons remains more difficult, requiring special approaches when choosing the initial data and accounting for all the features of the flow.

The study of the characteristics of shortened nozzles with bell-shaped nozzles was carried out by a team of authors at the Institute of Technical Mechanics of the National Academy of Sciences of Ukraine and the State Space Agency of Ukraine relatively long ago [12, 20]. The choice of the nozzle profile and tip length in the design of solid-fuel rockets is determined by the specific features of the rocket design, the conditions of the layout of the stages, etc. The design of a shortened nozzle with a tip should include several stages:

— selection of the base nozzle profile to which the nozzle is connected;

— determining the length of the base nozzle;

— construction of a tip that satisfies the design task (degree of expansion, length, shape, etc.);

— choosing the connection form of the tip with the basic nozzle.

Using a complex of programs simulating two-phase flow, taking into account coagulation, particle crushing, and the mutual influence of particles and gas, calculations of flow parameters in shortened nozzles of rocket engine of solid fuel with different degrees of expansion $F_a/F_* = 31.36,57.6,100$ at $\gamma = 1.166$ were carried out (F_a — area of the end section of the nozzle, F_* — critical cross-sectional area of the nozzle) [20]. Studies have shown that for all considered options, specific momentum losses are determined mainly by scattering losses ζ_p and solid phase (particles) lag ζ_d. Other loss components have a much smaller impact. From the point of view of nozzle momentum loss for reducing its length with the addition of various nozzles, more than 20 variants of contours with three basic nozzles were considered. Studies have shown that reducing the length of the supersonic base nozzle (in front of the nozzle) affects the components of momentum losses, namely, leads to increasing the maximum value of dispersion losses ζ_p and the presence of "two-phase" ζ_d. However, the first losses before the nozzle cut decrease, and the second — remains unchanged. Thus, it was established that in the direction of the cut of a shortened nozzle with a tip, the non-uniformity of the flow parameters slightly depends on the length of the initial base part of the nozzle, and the acceleration of the

particles is related to the character of the flow expansion into the nozzle.

The analysis of the components of the relative momentum losses in shortened nozzles with bell-shaped tips showed that the dependence of the relative scattering losses ζ_p on the relative length of the conical part $(x_a - x_н)/x_н$ of the nozzle is linear, and the two-phase losses ζ_d are correlated by the second-order parameter $(x_a - x_0)\ (x_н - x_0)/\ x_a^2$ (here x_a — the total length of the nozzle, x_0 — the length of the base nozzle, $x_н$ — the tip length). At the same time, relative scattering losses are almost three times higher than two-phase losses. Analysis of the change rate (along the nozzle length) of the relative momentum of the shortened nozzle showed that it increases with the decrease in the base nozzle length. With different tips and the same total length of the nozzle with the tip, the momentum coefficient (momentum coefficient — $K_i = I/(P_0F_*)$, where I — the nozzle momentum, P_0 — the total pressure at the nozzle inlet, F_* — the area of the critical section in the nozzle) practically does not change [20]. This indicates that the tip shape has an insignificant effect on the final value of the momentum coefficient. This important conclusion for modeling the contour of a shortened nozzle was confirmed in the authors' latest works, which were carried out based on the "ANSYS" software package [10, 11, 21]. The paper [10] showed a significant difference between the flow in a nozzle with a tip and the flow in a Laval nozzle profiled along the streamline of the same geometric degree of expansion but without a tip. The agreement of the calculations of the shortened nozzle characteristics with the experimental studies of the authors [12, 20] was also confirmed. The optimal flow turbulence model for the calculations of such flows was chosen, and the influence of gas properties on the calculation characteristics of the flow structure in non-traditional configurations was studied. The justification for choosing the turbulence model is presented by the authors in [21]. In [11], the traction characteristics of the flow in a bell-shaped nozzle were studied in detail: the pressure distribution on the tip wall and the traction characteristics of the nozzle with the tip. The geometric parameters of the nozzle significantly affect the wave nature of the flow in the nozzle and, accordingly, the impulse characteristics of the nozzle. The paper [22] shows the peculiarities of the wave flow structure in the analyzed class of shortened nozzles for the short conical part of the base nozzle.

The purpose of the work is to generalize the study results of supersonic flows in a shortened nozzle with a bell-shaped tip and analyze the effect of the base nozzle length, inlet and external pressure on the flow characteristics in the nozzle.

METHODS

The flow in a shortened nozzle with a bell-shaped tip of different lengths (formed by different lengths of the conical part of the base nozzle) is considered. Two variants were adopted based on the nozzle studied theoretically and experimentally in [8, 9].

The conical section (radius 5 mm) is followed behind the critical section of the Laval nozzle with a half-angle opening of 20° (Fig. 1). The transition of the conical section of the nozzle into the bell-shaped tip is carried out at the corner point. The length of the conical section of nozzle № 1 is 5 mm; nozzle № 2 is 20 mm. The nozzle exit has an angle of 0°. The total length of the shortened nozzle with tip is 35 mm. The nozzle wall radius at the exit is 28 mm. The geometric expansion ratio of the nozzle with the tip is $F_a/F_* = 31.36$.

The correctness of the initial condition choice (in particular, models of turbulence, physical properties of gas, etc.) was substantiated by results verification of simulating the gas flow in the Laval nozzle and in the base shortened nozzle with a conical part length of 10 mm with experimental operation [10]. The calculations are carried out in an axisymmetric setting using the ANSYS software package with the initial flow characteristics: ideal gas, isentropic index $\gamma = 1.4$, total flow temperature $T_0 = 300$ K. The

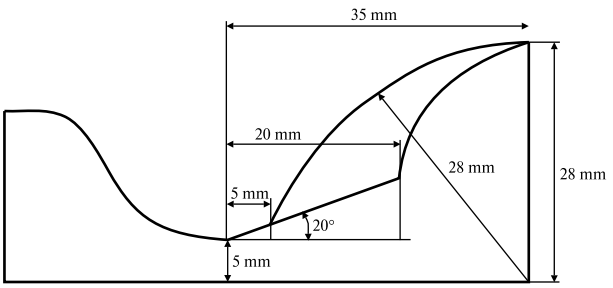

Figure 1. Contour of the nozzle with a long conical part l = = 5 mm (nozzle № 1) and l = 20 mm (nozzle № 2)

admissibility of the transition from the real flow of "hot" combustion products in the nozzles to "cold" gas is substantiated by comparing the results of calculation of the flow in the nozzle with experiments [10].

RESULTS AND DISCUSSIONS

This paper studies supersonic flows in shortened nozzles with a total length of the supersonic part of 35 mm with a long tip (nozzle № 1) and a short one (№ 2). These nozzles differ in the length of the conical part (5 and 20 mm) and the degree of distortion of the spherical contour of the nozzle. As a compression result, the spherical nozzle turns into a bell-shaped one. This compression affects the wave structure of the gas flow in the nozzle.

The nature of the flow in a shortened nozzle is affected by the conditions of its operation: launch at sea level and flight in the upper atmosphere. For the correct construction of the flow structure, it is necessary to consider the region not only inside the nozzle but also behind its exit section. In this regard, the computational area consists of two blocks, one of which is used to simulate the flow in the nozzle, and the other allows taking into account the outflow of the jet into the surrounding space.

The calculations were carried out in a non-stationary axisymmetric formulation based on the Reynolds-averaged Navier–Stokes equations with the kω-SST turbulence model [25], with near-wall functions and correction for compressibility. The choice of the mentioned turbulence model is due to the analysis carried out in [21] and the choice of the most optimal model for the flow in similar nozzles under study. To control the convergence of the iterative process, the level of discrepancy of the desired functions is checked. Calculations stop when the residual level of all necessary functions reaches 0.0001. The total number of iterations depends on the ambient conditions ($P_н$) and ranges from 400 to 800 iterations.

Figure 2 shows the isolines of the Mach numbers of flows in nozzle № 1 (*a*) and № 2 (*b*) at an inlet pressure $P_0 = 50 \cdot 10^5$ Pa at an ambient pressure $P_н = 1 \cdot 10^5$ Pa.

Supersonic flows in nozzles № 1 and № 2 have both similarities and differences. First of all, in both cases, a hanging shock 2 is formed in front of the free jet boundary 1. It is caused by supersonic compression of the characteristics reflected from the free boundary of the jet near the exit nozzle edge. This jump ends with a Mach disk 3, behind which the flow is already subsonic (region 5 in Fig. 1). The shape and length of the flow core up to the first Mach disk depend on the tip length. With a decrease in the tip length (an increase in the length of the inlet conical part of the nozzle), the jet core (the first "barrel") lengthens, and the size of the Mach disk 3 decreases.

Attention should be paid to the flow near the tip wall. Since the tip length of the nozzle № 2 was reduced by its compression, there is a great increase in the change in the tip radius near its exit, in contrast to the tip of the nozzle № 1. This fact affected the flow structure in the tip wall region and led to a change in the nozzle flow pattern in general. The transverse zone dimensions of developed flow separation from its wall behind the corner point 6 of the entrance to the tip in nozzle № 2 are much larger in comparison with one of nozzle № 1. In both cases, a large-scale vortex structure 7 is observed near the tip wall. Moreover, for a short tip (nozzle № 2), this vortex has a lower intensity and, accordingly, a higher pressure on the tip wall. In a long nozzle (nozzle № 1), there is a zone of secondary vortex 8, caused by an intense turn of the external flow into the tip (near its end) due to the smaller transverse dimensions of the flow separation region in the nozzle № 1 tip compared to the tone of nozzle № 2.

In the core of the gas jet, the flow accelerates unevenly, high velocities up to $M = 5.5$ are observed in the peripheral zone of the jet before the hanging shock 2. The structure of the Mach number isolines in both nozzles has a similar character. A characteristic hanging "saddle-shaped" shock 10 of low intensity is observed in the core of the gas flow behind the end of the inlet conical part of the nozzle (curved lines 11 of the Mach number isolines in Fig. 2).

As the ambient conditions change, the gas flow in the nozzles changes. Figure 3 shows the Mach number isolines in the gas flow at the inlet pressure $P_0 = 50 \cdot 10^5$ Pa and the ambient pressure $P_н = 0.1 \cdot 10^5$ Pa in nozzle № 1 (*a*) and № 2 (*b*).

At the walls of both nozzles, the flow is unseparated. From the corner point 1 of the tip entrance, a hanging shock 2 appears and extends to the tip end 3,

practically repeating the shape of the tip wall. However, in a long tip behind the hanging shock 2, a developed zone 4 of low velocity and high pressure is formed near the tip wall, caused by the reversal of the flow in the shock. Such a region is practically absent in the short tip № 2. This is explained by the large angle of flow inflow to the tip wall after turning at the corner point of entry into the tip. Further behind the tip end, the flow from zone 4 expands and forms zone 5. The jet flowing out of the high-pressure zone 4 deforms the hanging shock 2 of the first "barrel" of the supersonic flow just behind the tip end in zone 6. The free boundary 7 of the flow behind the tip end of both nozzles deviates from the axis by the angle determined by the Prandtl-Meyer flow at the corner point of the tip end. In both cases, an expanding flow zone 5 is formed. However, these zones differ (for the compared nozzles) in their shape and intensity (velocity and pressure). In nozzle № 2, the hanging shock 2 (with relatively greater intensity) pushes zone 5 into the free ambient space. In this case, the shock line itself moves away from the nozzle axis, and the flow velocity increases.

Figure 4 shows the distributions of flow Mach numbers in nozzles № 1 and 2 at an inlet pressure $P_0 = 50 \cdot 10^5$ Pa and $P_н = 0.1 \cdot 10^5$ Pa, which makes it possible to refine the behavior of the gas flow from the nozzle in the area of its end. As it can be seen, in the near trace behind the tip exit, the shape of the first "barrel" in both nozzle is significantly distorted in comparison with the case of flow at $P_0 = 50 \cdot 10^5$ Pa and $P_н = 1 \cdot 10^5$ Pa. In this case, just behind the tip end, there is a developed flow zone from the near-wall high-pressure layer (Fig. 7 below), formed behind the separated hanging shock 2 in front of the tip wall. The tip shape affects the flow deviation from the nozzle axis. In the case of a short nozzle (nozzle № 2), the flow deviates to a larger angle, which is explained by a large gradient in changing the tip shape. The flow reversal zone at the corner point of the tip end in the Prandtl-Mayer flow is practically not observed in comparison with the case of a long tip (nozzle № 1).

With a decrease in external pressure from $P_н = 0.1 \cdot 10^5$ Pa to $P_н = 0.01 \cdot 10^5$ Pa (Fig. 5), the wave nature of the flow in both nozzles practically does not change, except for an increase in the angle of devia-

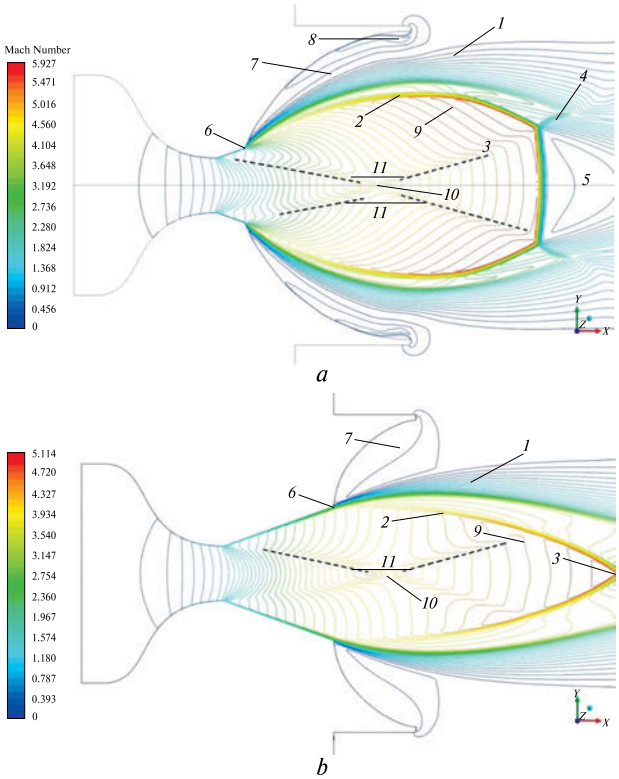

Figure 2. Isolines of the Mach numbers of the gas flow in nozzles № 1 and № 2 at inlet pressure $P_0 = 50 \cdot 10^5$ when operating at sea level ($P_н = 1 \cdot 10^5$ Pa)

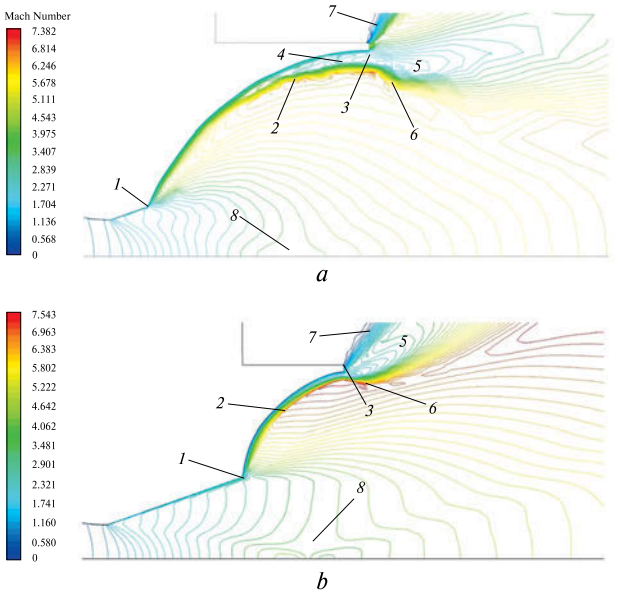

Figure 3. Isolines of the flow Mach numbers in nozzles № 1 and № 2 at inlet pressure $P_0 = 50 \cdot 10^5$ Pa when operating in the upper atmosphere ($P_н = 0.1 \cdot 10^5$ Pa)

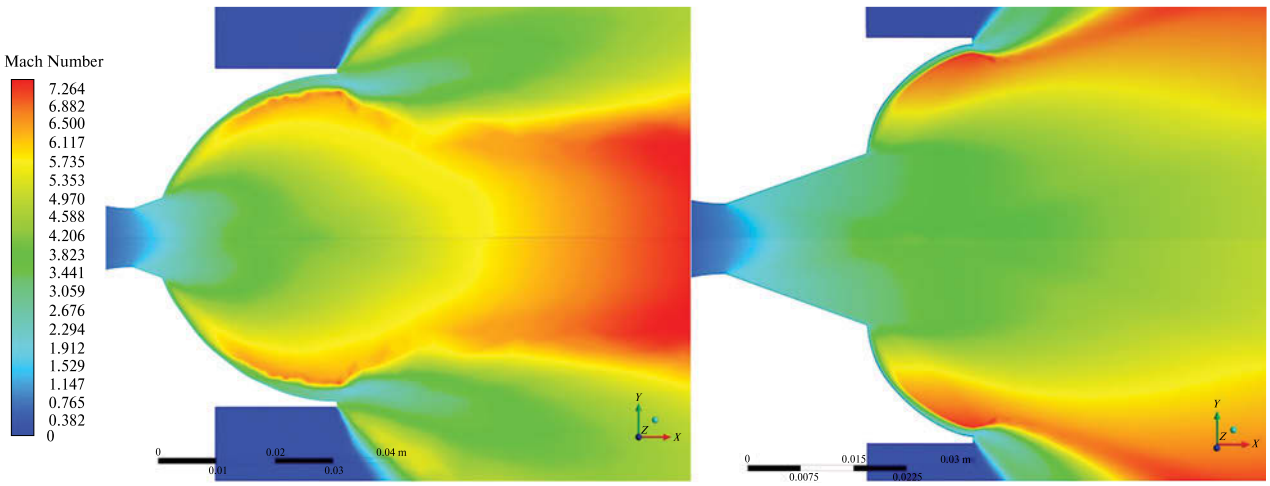

Figure 4. Distribution of Mach numbers of flows in nozzles № 1 (*a*) and № 2 (*b*) at inlet pressure $P_0 = 50 \cdot 10^5$ Pa when operating in the upper atmosphere $P_н = 0.1 \cdot 10^5$ Pa

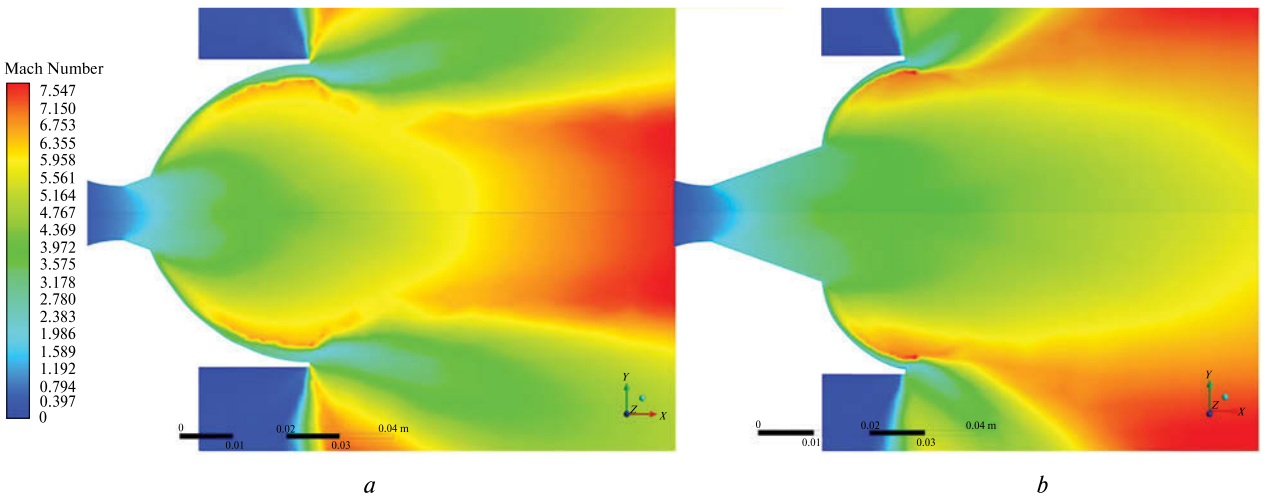

Figure 5. Distribution of flow Mach numbers in nozzles № 1(*a*) and № 2 (*b*) at inlet pressure $P_0 = 50 \cdot 10^5$ Pa when operating in the upper atmosphere of $P_н = 0.01 \cdot 10^5$ Pa

tion of the free boundary of the flow in accordance with a decrease in external pressure. One can note a more developed Prandtl-Meyer flow at the corner point of the nozzle with the above features for nozzles № 1 and № 2.

Simulation of the flow in a nozzle with a short tip with an increase in inlet pressure up to $P_н = 100 \times \times 10^5$ Pa (Fig. 6) showed that the wave structure of the flow is similar to the flow structure at $P_0 = 50 \cdot 10^5$ Pa.

As for the flow at $P_0 = 50 \cdot 10^5$ Pa (Fig. 2, *b*), for the flow at sea level at $P_0 = 100 \cdot 10^5$ Pa, a hanging "saddle-shaped" shock of low intensity and a clearly expressed first "barrel" are observed near the nozzle axis. There is also a zone of developed flow separation behind the corner point of entry into the tips with a large vortex.

For the flow in the upper layers of the atmosphere, $P_н = 0.1 \cdot 10^5$ Pa, with an increase in inlet pressure,

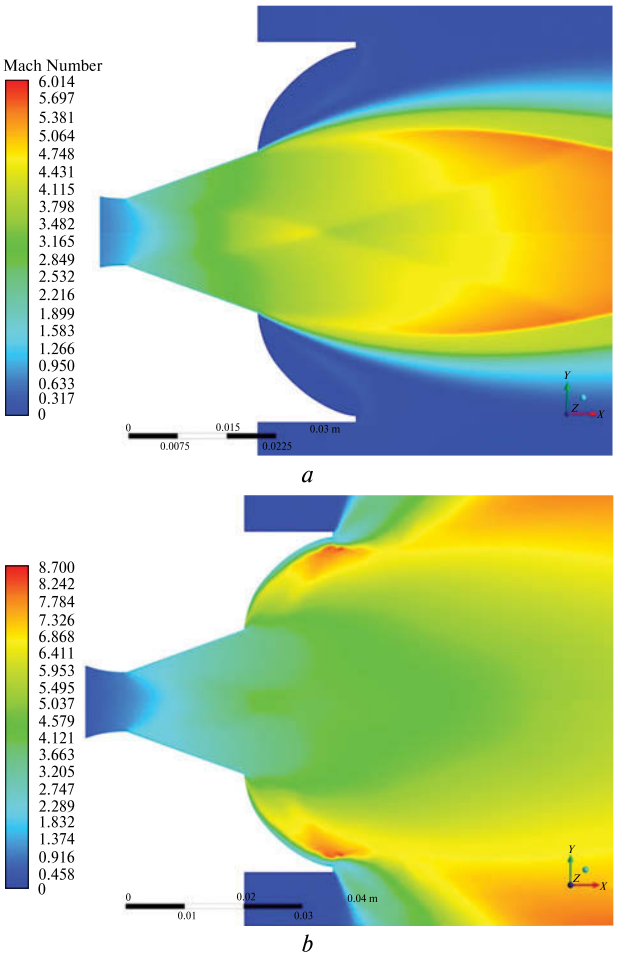

Figure 6. Distribution of flow Mach numbers in nozzle № 2 at inlet pressure $P_0 = 100 \cdot 10^5$ Pa when operating at sea level $P_н = 1 \cdot 10^5$ Pa (*a*) and in the upper atmosphere (*b*) at $P_н = 0.1 \cdot 10^5$ Pa

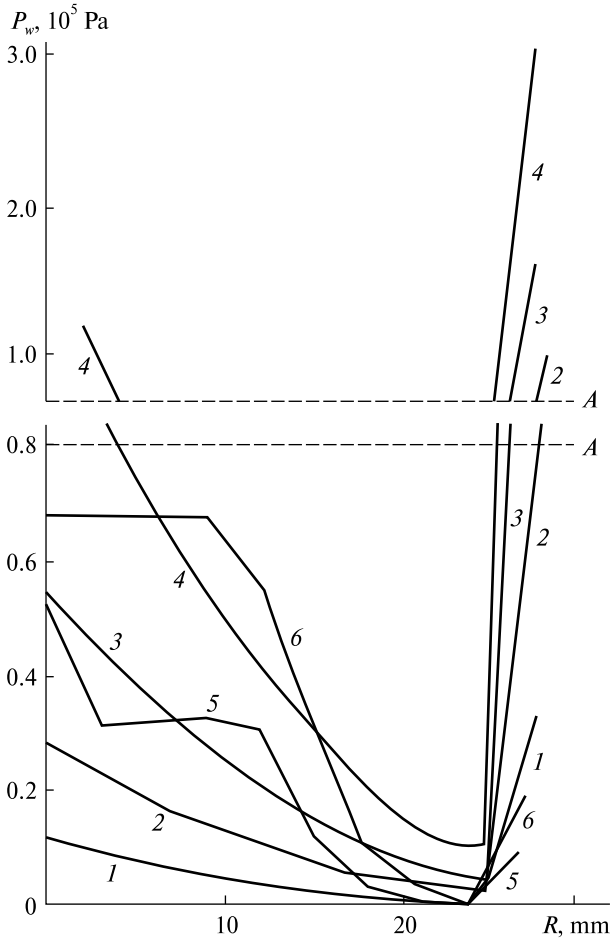

Figure 7. Distribution (along the radius) of the static pressure at the end of the shortened nozzle № 1 (curves *1—4*) and № 2 (curves *5—6*) with an external pressure $P_н = 0.1 \cdot 10^5$ Pa and inlet pressure $P_0 = 20 \cdot 10^5$ Pa (curve *1*), $50 \cdot 10^5$ Pa (curve *2* and *5*), $100 \cdot 10^5$ Pa (curve *3* and *6*), $200 \cdot 10^5$ Pa (curve *4*)

it's observed (as in the case of $P_0 = 50 \cdot 10^5$ Pa, Fig. 4, *b*) a change in the shape of the first "barrel" and the absence of a hanging "saddle-shaped" shock of low intensity in the flow core.

The difference between the flow at $P_0 = 100 \times \times 10^5$ Pa and the flow at $P_0 = 50 \cdot 10^5$ Pa consists mainly of a larger deviation behind the tip exit of the free flow boundary. There is also a slight difference in the structure of the flow outflowing from the high-pressure zone behind the detached shock in front of the tip wall.

Figures 7 and 8 show the distribution (along the nozzle radius) of the static pressure at the exit of the shortened nozzles № 1 and № 2 at different inlet pressure values and the pressure of the ambient space.

According to the distribution of static pressure on the tip end of nozzle № 1 and № 2 (Fig. 7) at pressures in front of the nozzle $P_0 = 20 \cdot 10^5$ Pa, $50 \cdot 10^5$ Pa, $100 \cdot 10^5$ Pa, and $200 \cdot 10^5$ Pa and at an external pressure $P_н = 0.1 \cdot 10^5$ Pa, it can be seen that the nature of the flow in the core is different for nozzles with different tip. For a nozzle with a long tip, the static pressure P_w monotonically decreases in all cases from the nozzle axis to the "inflection" point $0.9\bar{R} = 0.9 \cdot R/R_a$, where R is the current radius value, $R_a = 28$ mm is the tip wall radius at the outlet. As

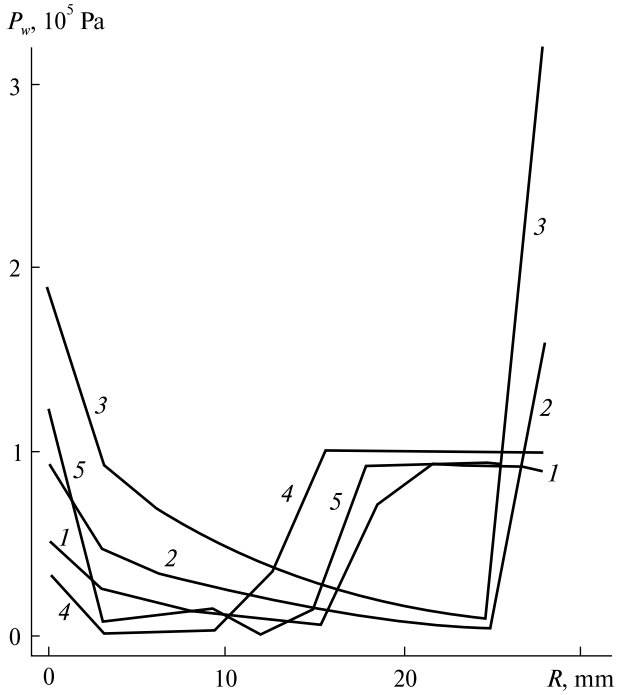

Figure 8. Distribution of flow static pressure (along the radius) at the end of the shortened nozzle № 1 (curves *1—3*) and № 2 (curves *4—5*) with external pressure $P_н = 1.0 \cdot 10^5$ Pa and inlet pressure $P_0 = 50 \cdot 10^5$ Pa (curves *1* and *4*), $100 \cdot 10^5$ Pa (curves *2* and *5*), $200 \cdot 10^5$ Pa (curves *3* and *6*)

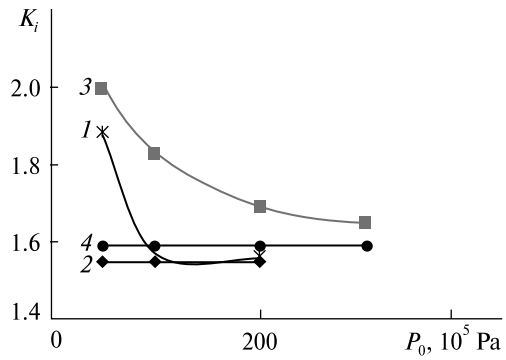

Figure 9. Impulse coefficients for nozzles № 1 and № 2 under different operating conditions: *1* — $l = 5$ mm, $P_н = 1 \cdot 10^5$ Pa; *2* — $l = 5$ mm, $P_н = 0.1 \cdot 10^5$ Pa; *3* — $l = 20$ mm, $P_н = 1 \cdot 10^5$ Pa; *4* — $l = 20$ mm, $P_н = 0.1 \cdot 10^5$ Pa

R increases, the pressure increases linearly up to a maximum value. In a nozzle with a short tip (nozzle № 2), the pressure from the axis decreases no monotonically (curves *5–6* in Fig. 7), regions of constant pressure are observed, and the pressure level is proportional to the value of the inlet pressure. Further beyond the specified "inflection" point on the section, the pressure increases monotonically, but it is much less than for nozzle № 1. This character of the pressure distributions on the tip end correlates with the flow patterns in the nozzles given above.

Figure 8 shows the distribution of static pressure at the tip end section of nozzles № 1 and № 2 along the radius *R* when operating at sea level $P_н = 1 \cdot 10^5$ Pa and inlet pressures $P_0 = 50 \cdot 10^5$ Pa, $100 \cdot 10^5$ Pa and $200 \cdot 10^5$ Pa.

The nature of the curves in Fig. 8 is slightly different from the corresponding curves in Fig. 7. For nozzle № 1 at $P_0 = 50 \cdot 10^5$ Pa, the flow pressure from the nozzle axis to the point $\bar{R} \approx 0.55$ (curve *1*) decreases monotonically, then to $\bar{R} \approx 0.8$ it increases to $0.85 \cdot 10^5$ Pa, after that it decreases slightly (to $0.82 \times \times 10^5$ Pa) to the tip end. At $P_0 = 100 \cdot 10^5$ Pa (curve *2*) and $200 \cdot 10^5$ Pa (curve *3*), the change in pressure along the radius at the tip exit is monotonous and similar to the change one at $P_н = 0.1 \cdot 10^5$ Pa (Fig. 7) with a slight change in the gradient at the point $\bar{R} \approx 0.11$.

For a short tip (nozzle № 2), the pressure distribution on its end section has no monotonic character. From the nozzle axis to the first point of monotony change $\bar{R} \approx 0.11$, the pressure decreases monotonically (curves *4*, *5*) with a gradient proportional to the inlet flow pressure. Next, there is a region of constant pressure up to $\bar{R} \approx 0.32$ (curve *4*) and $\bar{R} \approx 0.43$ (curve *5*). With a further increase in the radius to $\bar{R} \approx 0.57$ (curve 4) and $\bar{R} \approx 0.64$ (curve *5*), the pressure increases monotonically. After that, the pressure does not change with increasing radius ($P_w \approx 0.9 \cdot 10^5$ Pa at $P_0 = 100 \cdot 10^5$ Pa and $P_w \approx 0.97\ 10^5$ Pa at $P_0 = = 50 \cdot 10^5$ Pa).

This character of the flow pressure distribution coincides with the distribution of the flow Mach numbers considered above (Fig. 2).

The analysis of impulse coefficients confirmed the conclusion about the influence of the conical part length of the shortened nozzle on impulse coefficients. In Fig. 9, curves *1* and *2* correspond to the impulse coefficient value of the shortened nozzle № 1 with a short conical part ($l = 5$ mm), curves *3* and *4* — K_i for nozzle № 2 ($l = 20$ mm). As the length of the conical part of the nozzle decreases, the im-

pulse coefficient decreases significantly during operation only at sea level (by 9.1—10.2 %) and slightly decreases during operation in the upper layers of the atmosphere (by 2.5 %). This nature of the change in impulse characteristics is explained by the change in the wave structure of the flow in the middle of the nozzle. An increase in the size of the developed separation flow zone (Fig. 2) in a nozzle with an elongated nozzle and, correspondingly, reduced sizes of the conical nozzle part leads to a loss of impulse. This coincides with the conclusion that was made earlier based on calculations of impulse characteristics of flows in shortened nozzles by approximating methods and experimental studies of flows in shortened nozzles [20].

CONCLUSIONS

A comparison of the wave structures of a supersonic gas flow is made in shortened nozzles with the same total length and with different lengths of tips formed by compression and stretching of the original bell-shaped tip for connecting with the long and short conical part of the base nozzle, respectively. Under operating conditions at sea level and pressure at the nozzle inlet $P_0 < 50 \cdot 10^5$ Pa, a large-scale vortex structure is observed in both nozzles, starting from the corner entry point into the nozzle. In a long nozzle, in addition, a small-scale vortex is observed on the wall near its end. A barrel-shaped wave structure of hanging shocks with a closing Mach disk is formed in the flow in both nozzles, inside which a "saddle-shaped" wave structure of low intensity is observed. In the case of separated flow in the tip (at $P_0 < 50 \cdot 10^5$ Pa and $P_н = 1 \cdot 10^5$ Pa), the pressure on its wall in the separation zone is a little lower (by ≈ 5—10 %) than the external pressure $P_н$.

The static pressure in the cross-section at the tip end of both nozzles is proportional to the pressure at the nozzle inlet operating in the upper layers of the atmosphere. From the nozzle axis to the point $\sim 0.89R/R_a$, the pressure decreases to a value corresponding to the pressure at the nozzle inlet. It then increases linearly to the nozzle wall flow pressure, which is also proportional to the nozzle flow inlet pressure. This is explained by the wave structure of the flows in the middle of the nozzles.

As the length of the conical nozzle part decreases, the impulse coefficient decreases significantly when operating at sea level and slightly decreases when operating in the upper layers of the atmosphere. The results of the calculations correlate satisfactorily with the conclusions obtained during experimental studies of flows in shortened nozzles with bell-shaped nozzles.

REFERENCES

1. Arora R., Vaidyanathan A. (2015). Experimental investigation of flow through planar double divergent nozzles. *Acta Astronomica*, **112**, 200—216.
2. Asha G., Naga Mohana D., Sai Priyanka K., Govardhan D. (2021). Design of minimum length nozzle using method of characteristics. *Int. J. Engineering Res. and Technology (IJERT)*, **10**, № 5, 490—495.
3. Emelyanov V. N., Volkov K. N., Yakovchuk M. S. (2022). Unsteady flow in a dual-bell nozzle with displacement of an extendible section from the initial to working position. *Fluid Dynamics*, **57** (Suppl. 1), 35—45.
4. Genin C., Stark R., Haidn O., Quering K., Frey M. (2013). Experimental and numerical study of dual bell nozzle flow. *Progr. Flight Phys.,* **5**, 363—376.
5. Génin Ch., Stark R. (2010). Experimental study on flow transition in dual bell nozzles. *J. Propulsion and Power*, **26**, 497—502.
6. Gogish L. V. (1966). Investigation of short supersonic nozzles. *Izvestiya Akademii nauk SSSR. Mehanika zhidkosti i gaza*, № 2, 175—180 [in Russian]
7. Hagemann G., Frey M., Koschel W. (2002). Appearance of restricted shock separation in rocket nozzles. *J. Propulsion and Power*, **18**, 577—584.
8. Hamitouche T., Sellam M., Kbab H., Bergheul S. (2019). Design and Wall Fluid Parameters Evaluation of the Dual-Bell Nozzle. *Int. J. Engineering Res. and Technology*, **12**, № 7, 1064—1074.
9. Hunter C. A. (2004). Experimental, theoretical and computational investigation of separated nozzle flows. *Proc. 34th AIAA/ASME/SAE/ASEE Joint Propulsion Conf. and Exhibition* (Cleveland, 2004). Paper № 1998-3107, 1—10.
10. Ihnatiev O. D., Pryadko N. S., Strelnikov G. O., Ternova K. V. (2022). Gas flow in a shortened Laval nozzle with a bell-shaped nozzle. *Technical mechanics*, № 2, 39—46.
11. Ihnatiev O. D., Pryadko N. S., Strelnikov G. O., Ternova K. V. (2022). Thrust characteristics of a truncated Laval nozzle with a bell-shaped tip. *Technical mechanics*, № 3, 35—46.
12. Kovalenko N. D., Strelnikov G. A., Gora Yu. V., Grebenyuk L. Z. (1993). *Gas dynamics of supersonic shortened nozzles*. Kyiv: Naukova dumka, 223 p. [in Russian]
13. Kumar M., Fernando D., Kumar R. (2013). Design and optimization of de Lavel nozzle to prevent shock induced flow separation. *Advs in Aerospace Sci. and Applications*, **3**, № 2, 119—124.
14. Narayan A., Panneerselvam S. (2012). Study of the effect of over-expansion factor on the flow transition in dual bell nozzles. *Int. J. Mech. AerospaceInd. Mechatron. Manuf. Eng.*, **6**, № 8, 1591—1595.
15. Nasuti F., Onofri M., Martelli E. (2005). Role of wall shape on the transition in axisymmetric dual-bell nozzles. *J. Propul. Power*, **21**, №. 2, 243—250.
16. Rao G. V. R. (1958). Exhaust Nozzle Contour for Optimum Flight. *Jet Propulsion*, **28**, № 6, 377—382.
17. Sergienko A. A., Sobachkin A. A. (1990). Profiling of short supersonic round nozzles. *Izd. vuzov. Aviats. Tehnika*, № 2, 62—64 [in Russian]
18. Sreenath K. R., Mubarak A. K. (2016). Design and analysis of contour bell nozzle and comparison with dual bell nozzle. *Int. J. Res. Eng.*, **3**, № 6, 52—56.
19. Stark R., Genin C., Wagner B., Koschel W. (2012). The altitude adaptive dual bell nozzle. *Proc. 16th Int. Conf. On the Methods of Aerophys. Res.* (ICMAR 2012), 1—8.
20. Strelnikov G. A. (1993). *Adjustable short supersonic nozzles.* Dnepropetrovsk: DGU, 191 p. [in Russian]
21. Strelnikov G., Pryadko N., Ihnatiev O., Ternova K. (2022). Choice of a turbulence model for modeling complex flows in rocket engine nozzles. *Novel Res. in Sci.,* **10**, № 5, 1—4.
22. Strelnikov G. A., Pryadko N. S., Ternova K. V. (2023). Wave structure of the gas flow in a shortened nozzle with a long bell-shaped tip. *Techn. mechanics*, № 1, 14—23.
23. Taylor N., Steelant J., Bond R. (2011). Experimental comparison of dual bell and expansion deflection nozzles. *Proc. 47th AIAA/ASME/SAE/ASEE Joint Propulsion Conf. & Exhibition* (SanDiego. 2011). Paper № 2011-5688, 1—13.
24. Vermaa S. B., Haidnb O. (2014). Unsteady shock motions in an over-expanded parabolic rocket nozzle. *Aerospace Sci. and Technology*, **39**, 48—71.
25. Wilcox D. (2006) *Turbulence Modeling for CFD*. California : DCW Industries, Inc., 536 p.

Стаття надійшла до редакції 07.04.2023 *Received 07.04.2023*
Після доопрацювання 25.05.2023 *Revised 25.05.2023*
Прийнято до друку 28.10.2023 *Accepted 28.10.2023*

Н. С. Прядко, проф., д-р техн. наук, пров. наук. співроб.
ORCID 0000-0003-1656-1681
E-mail: np-2006@ukr.net
Г. О. Стрельников, проф., д-р техн. наук, в.о. зав. відділу
ORCID 0000-0001-9810-1966
E-mail: strelaga38@ukr.net
К. В. Тернова, канд. техн. наук, старш. наук. співроб.
ORCID 0000-0001-9560-5827
E-mail: ternovayakaterina@gmail.com

Інститут технічної механіки Національної академії наук України і Державного космічного агентства України
вул. Лешко-Попеля 15, Дніпро, Україна, 49005

ДОСЛІДЖЕННЯ НАДЗВУКОВОГО ПОТОКУ В УКОРОЧЕНИХ СОПЛАХ РАКЕТНИХ ДВИГУНІВ ІЗ ДЗВОНОПОДІБНИМ НАСАДКОМ

Розглядається течія в укороченому соплі з дзвоноподібним насадком. Проведено порівняння хвильових структур надзвукового потоку газу в укорочених соплах з коротким і довгим насадками, утвореними стисненням і розтягуванням вихідного дзвоноподібного насадка для з'єднання, відповідно, з довгою та короткою конічною частиною базового сопла при однаковій довжині сопла. В умовах роботи на рівні моря та малому тиску на вході в сопло ($P_0 < 50 \cdot 10^5$ Па) в обох насадках спостерігається великомасштабна вихрова структура, що починається від кутової точки входу в насадок. У довгому насадку, крім цього, спостерігається дрібномасштабний вихор на стінці біля його зрізу. У потоці в обох насадках формується бочкоподібна хвильова структура висячих стрибків із замикаючим диском Маха, усередині якої спостерігається сідлоподібна хвильова структура малої інтенсивності. При відривній течії в насадку (при $P_0 < 50 \cdot 10^5$ Па і $P_н = 10^5$ Па) тиск на стінці в зоні відриву дещо нижчий (на 5...10 %) від зовнішнього тиску $P_н$. При роботі двигуна у верхніх шарах атмосфери статичний тиск на зрізі обох насадків пропорційний до тиску на вході в сопло. У поперечному перерізі, починаючи від осі сопла до $0.89R/R_a$ (відношення поточного значення радіуса R до радіуса стінки насадка на виході R_a) тиск зменшується до значення, пропорційного тиску на вході в сопло. Потім він лінійно збільшується до значення тиску на стінці насадка, який пропорційний тиску на вході в сопло. Це пов'язано з хвильовою структурою потоку всередині насадка. Встановлено, що із зменшенням довжини конічної частини сопла коефіцієнт імпульсу сопла зменшується суттєво при роботі на рівні моря та незначно зменшується при роботі у верхніх шарах атмосфери. Результати розрахунків задовільно корелюють з результатами експериментальних досліджень течій у вкорочених соплах із дзвоноподібним насадком.

Ключові слова: укорочене сопло, насадок, надзвуковий потік, тиск, хвильова структура, імпульс.